arXiv:1409.7104v1 [cond-mat.str-el] 24 Sep 2014

Collective impurity effects in the Heisenberg triangular antiferromagnet

V S Maryasin[1] and M E Zhitomirsky[2]

[1] University Grenoble-Alps and INAC-SPSMS, F-38000 Grenoble, France
[2] Service de Physique Statistique, Magnétisme et Supraconductivité, INAC, CEA, 17 rue des Martyrs, 38054 Grenoble Cedex 9, France

E-mail: vladimir.maryasin@cea.fr, mike.zhitomirsky@cea.fr

Abstract. We theoretically investigate the Heisenberg antiferromagnet on a triangular lattice doped with nonmagnetic impurities. Two nontrivial effects resulting from collective impurity behavior are predicted. The first one is related to presence of uncompensated magnetic moments localized near vacancies as revealed by the low-temperature Curie tail in the magnetic susceptibility. These moments exhibit an anomalous growth with the impurity concentration, which we attribute to the clustering mechanism. In an external magnetic field, impurities lead to an even more peculiar phenomenon lifting the classical ground-state degeneracy in favor of the conical state. We analytically demonstrate that vacancies spontaneously generate a positive biquadratic exchange, which is responsible for the above degeneracy lifting.

1. Introduction

Due to inherent competition of the principal interactions, frustrated magnets are susceptible to effects at much lower energy scales that are determined by additional interactions, fluctuations, or structural disorder. Though, the first two sources of degeneracy lifting have been extensively studied in the literature, resulting in a wide range of theoretical models, a detailed phenomenology of the impurity effects on frustrated magnets is lacking so far. Most of the existing studies focus on a single impurity problem. These include magnetic susceptibility of an impurity [1–3], spin renormalization and screening patterns around an impurity [4–7] and partial relief of frustration [8].

In this work we study the effect of dilution with nonmagnetic impurities on the paradigmatic frustrated model of the Heisenberg triangular-lattice antiferromagnet (TAFM) [9,10]. We predict two essentially collective impurity phenomena, which develop only at finite concentration of defects $n_{\rm imp}$. The considered spin Hamiltonian is an isotropic classical antiferromagnet on a triangular lattice:

$$\hat{\mathcal{H}} = J\sum_{\langle ij\rangle} \mathbf{S}_i\cdot\mathbf{S}_j(1-p_i)(1-p_j) - \mathbf{H}\cdot\sum_i \mathbf{S}_i(1-p_i). \qquad (1)$$

Impurities are introduced via the parameter p_i, which is set to $p_i = 0$ on regular sites and to $p_i = 1$ on impurity sites, hence, $p_i^2 = p_i$. Impurities are assumed to be randomly distributed over the lattice and $\sum_i p_i = N_{\rm imp}$.

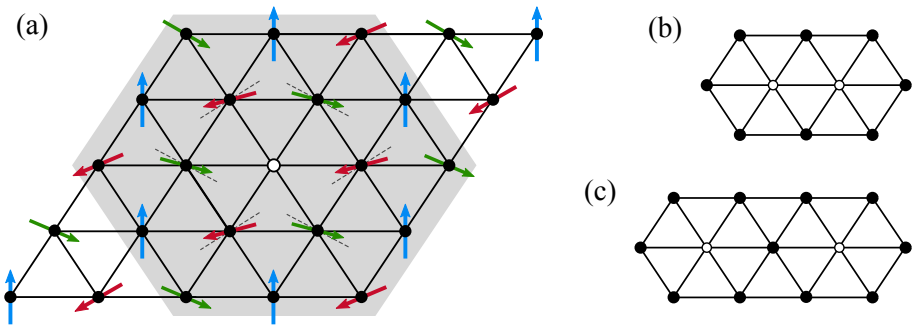

Figure 1. (a) An example of spin distortions around the impurity in the classical 120° ordered state. Shaded area shows all nearest neighbours up to the order 3. (b), (c) Simple clusters of impurities with the strongest distortion of screening. Effective magnetic moment of these configurations equals to $m_{\rm imp}^{\circ\circ} = 0.11$ and $m_{\rm imp}^{\circ\cdot\circ} = 0.08$ respectively.

Our first result is a nontrivial dependence of an effective impurity moment on the fraction of vacant sites $n_{\rm imp}$. In noncollinear magnets even in the absence of external magnetic field an impurity induces transverse local field on its neighbors and leads to the screening of magnetic moment of a missing spin. Wollny *et al.* [6] found that in the Heisenberg TAFM the magnetic moment around a vacancy is equal to $m_{\rm imp}^{\circ} = 0.039S$.

Here we report a substantial growth of the effective moment of a single impurity at finite concentrations of vacancies, observed in our numerical simulations. This growth is significant even at low concentrations $n \leqslant 1\%$, causing deviations from independent impurity behavior with $m_{\rm imp} = m_{\rm imp}^{\circ}$. We explain it by the effects of clustering of impurities. The results of our numerical simulations, as well as the details of numerical methods, used in this study are presented in the section 2.

The second effect of impurities considered in the present work is lifting of the continuous ground state degeneracy of the Heisenberg TAFM in an external magnetic field. This degeneracy gives rise to a rich phase diagram with various coplanar states [9–11] that can be understood theoretically using the concept of order by disorder. In our recent article [12] we have obtained numerically that vacancies doped into TAFM stabilize the conical ground state. Such a selection takes place because of a positive biquadratic exchange produced by structural disorder. The concept of an effective biquadratic exchange generated by quenched disorder in magnetic solids was first suggested by Slonczewski in the context of magnetic multilayers [13]. In our previous work on an impure TAFM [12] we have derived analytically a positive biquadratic exchange in a model with weak bond randomness, see also [14]. In Sec. 3 we generalize the previous analytic results by showing that the effective biquadratic exchange follows also from a weak site disorder.

2. Effective impurity moment

A removed magnetic moment in an antiferromagnetic insulator induces a net magnetic moment in the system. For noncollinear magnetic structures the moment is, however, screened by a spin texture resulting from the canting of the surrounding spins [5–7]. Such a spin canting of only nearest neighbor spins is illustrated in Fig. 1(a). As a result, an impurity moment acquires a non-universal fractional value, which depends on the system details. Wollny and collaborators [6] have shown that a vacancy in the classical Heisenberg TAFM becomes slightly overcompensated, i.e. at $T = 0$ the net magnetic moment is equal to $m_{\rm imp}^{\circ} = 0.039S$ and has the *same* direction as a missing spin. At finite temperatures in the absence of long range order this purely classical moment is free to rotate in spin space leading to a Curie-like paramagnetic divergence of the magnetic susceptibility at $T \to 0$. In a system with a small but finite concentration of impurities,

the impurity contributions sum up to give

$$\chi(T) = \frac{N_{\rm imp} m_{\rm imp}^2}{3T} + O(1). \tag{2}$$

In this section we consider dependence of the effective impurity moment $m_{\rm imp}$ on the impurity concentration $n_{\rm imp}$. We have numerically investigated a finite system with a fixed finite concentration of vacancies, measured $m_{\rm imp}$ and studied how the impurity screening is modified at finite $n_{\rm imp}$.

First we report results of Monte Carlo simulations of the classical nearest-neighbor Heisenberg antiferromagnet (1) on rhombohedral $L \times L$ clusters with finite concentration of static vacancies. Basically, we use the same algorithm, as in the previous works [11, 12]. We found that cluster size has little effect on bulk thermodynamic quantities at $T \to 0$ and, therefore, used moderate cluster size $L = 90$ in all runs for this work, except for the cases of small amount of impurities $n_{\rm imp} < 0.01$, where larger clusters are needed for better statistics.

Figure 2(a) shows the uniform magnetic susceptibility $\chi(T)$ normalized per spin obtained from the Monte Carlo simulations of the TAFM with and without impurities as

$$\chi = \frac{1}{3TL^2} \Big\langle \Big(\sum_i \mathbf{S}_i \Big)^2 \Big\rangle. \tag{3}$$

The main difference between the curves is the emergent $1/T$ divergence of χ at low temperatures, which becomes stronger with increasing $n_{\rm imp}$. This upturn may look counterintuitive as no extra magnetic moments are brought into the system. Note that our Monte Carlo results for $\chi(T)$ closely resemble the susceptibility data measured for nominally pure TAFM materials, for example, for $LuMnO_3$ [15].

We associate an average magnetic moment $m_{\rm imp}$ with every impurity and interpolate the susceptibility curves at $T \to 0$ with Eq. (2) to determine its value. In addition, we obtain independent results for the impurity moments $m_{\rm imp}$ by another method: direct calculation of

$$m_{\rm imp}^2 = \frac{1}{N_{\rm imp}} \Big(\sum_i \mathbf{S}_i \Big)^2 \tag{4}$$

in the classical ground state at zero temperature. The algorithm of the search of the ground state has been described in details in the works [12, 14]. Note that $m_{\rm imp}$, obtained by both methods was averaged over at least 200 random impurity configurations.

Figure 2(b) presents the main result of this section: a nontrivial growth of single impurity moment with concentration. Values, obtained by the two methods (displayed by full and open circles respectively) match perfectly and in the following we do not make the difference between the two methods. The growth is observed even at small $n_{\rm imp} \sim 1\%$, which is somewhat surprising as at such weak dilution one may expect a nearly independent impurity behavior with $m_{\rm imp} = m_{\rm imp}^{\circ}$. Indeed, Fig. 2 (b) shows that $m_{\rm imp}$ is significantly renormalized from the single impurity value, even at the lowest considered $n_{\rm imp} = 0.2\%$, which is comparable to the case of a single impurity on a cluster with $L = 12$, studied in the work of Wollny *et al.* [6].

One possible explanation of growing $m_{\rm imp}$ is an assumption that screening clouds from different impurity sites interact, and self-average. According to Ref. [6, 16] readjustment angles of spins, surrounding an impurity decay as $\delta\Theta(r) \sim 1/r^3$ at long distances. For a finite concentration of impurities one may expect cut off of individual screening clouds at average distances $R \sim n_{\rm imp}^{-1/2}$. It leads to the modification of screening, consistent with the square root dependence on vacancy fraction:

$$\delta m \sim \int \Theta(r) |\mathbf{l}(r)| d^2 r \sim n_{\rm imp}^{1/2}. \tag{5}$$

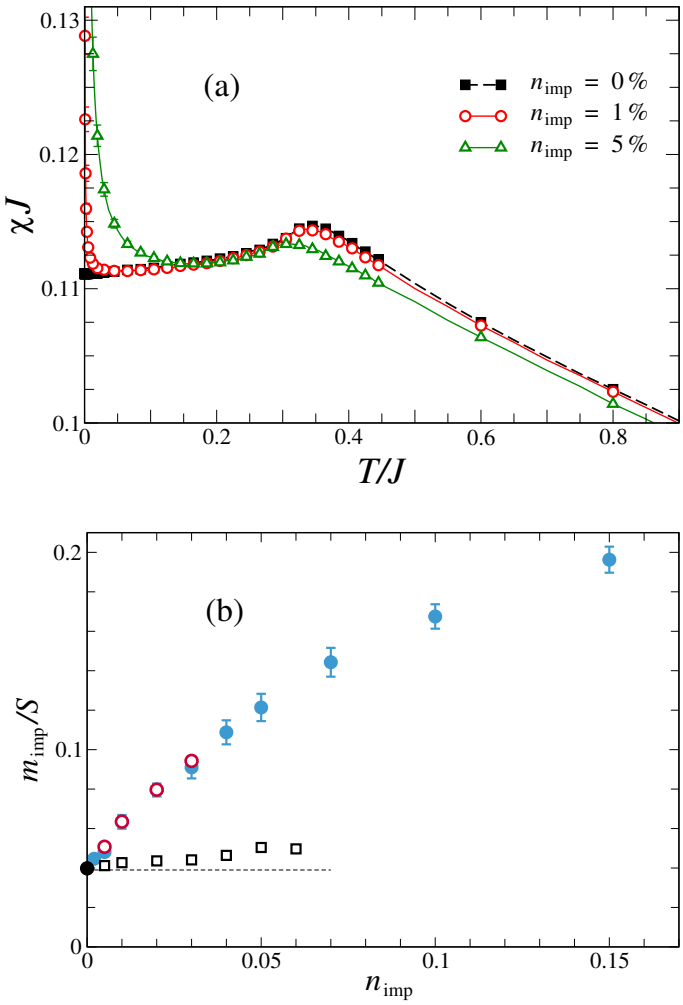

Figure 2. (a) Magnetic susceptibility for different concentrations of vacancies, from our Monte Carlo simulations. The Curie-like singularity at $T \to 0$ gives the value of effective impurity moment $m_{\rm imp}$. (b) Growth of effective vacancy moment with vacancy concentration obtained using susceptibility interpolation (full circles) and direct measurement at the ground state (open circles). Open squares correspond to simulation of the system with impurities, distributed at a distance from each other. Dashed line and a big marker at $n_{\rm imp} = 0$ show $m^{\circ}_{\rm imp}$ obtained in the work [6].

Here $\mathbf{l}(r)$ - is a vector, pointing in the direction spin distortion, and results only in a prefactor, which is omitted. However, the measured $m_{\rm imp}$ (fig. 2 (b)) does not fit to this procedure, and therefore demands for different explanation of the observed dependence.

We ascribe growth of impurity moment to the effects that are quadratic in $n_{\rm imp}$. Indeed, an individual impurity moment is strongly screened to a very small value $m^{\circ}_{\rm imp}$. Hence, one is forced to consider statistically rare cases of two impurities occupying nearby sites, see Figs. 1(b) and (c). If such impurity configurations have moments, which are not very well screened and which are significantly larger than $m^{\circ}_{\rm imp}$, their impact on the net magnetic moment and the low-temperature susceptibility may be quite significant.

We measured $m_{\rm imp}$ for a few simple vacancy configurations and show in Figs. 1(b) and (c) two impurity clusters with the largest values of the effective magnetic moment. The calculations

yield $m^{\circ\circ}_{\rm imp} = 0.11$ and $m^{\circ\cdot\circ}_{\rm imp} = 0.08$ respectively, the result, that is several times larger, than $m^{\circ}_{\rm imp}$. Along with the large coordination number of the triangular lattice, it overcomes the small statistical weight $P \sim n^2_{\rm imp}$ of these configurations.

In addition, we have performed similar numerical simulations restricting vacancies from being placed within the first three neighbors from each other. The respective exclusion region is is shown by the shaded area in Fig. 1(a). In the first place, such a computation serves to verify the above hypothesis; second it may also model weak correlations in the structural disorder, which develop in real solids due to elastic tension etc. The results are plotted in Fig. 2(b) with open square markers. They demonstrate only a slight growth of $m_{\rm imp}$ from $m^{\circ}_{\rm imp}$. Therefore, at distances exceeding 2–3 lattice spacings, impurities only barely interact and behave completely individually. These results strongly support the above explanation of the growth of impurity moment due to clustering of vacancies.

3. Disorder induced biquadratic exchange

In this section we elaborate on the mechanism of the degeneracy lifting in the TAFM as well as in a wide class of frustrated models produced by nonmagnetic impurities. In finite magnetic fields $0 < H < H_{\rm sat}$ the TAFM exhibits continuous degeneracy of ground states obeying the classical constraint $\mathbf{S}_{\triangle} = \mathbf{H}/3J$. Thermal [9, 10] and quantum [17] order by disorder are responsible for selecting the most collinear spin configurations. These include the coplanar 'Y' and '2:1' states below and above $\frac{1}{3}H_{\rm sat}$, respectively, and the collinear up-up-down state at the 1/3 magnetization plateau. The resulting complex phase diagram of the classical Heisenberg TAFM was obtained from the Monte Carlo simulations in [11]. At the phenomenological level, such a selection can be straightforwardly explained by appearance of an effective biquadratic exchange with negative sign: $-(\mathbf{S}_i{\cdot}\mathbf{S}_j)^2$. Such term was indeed obtained in the lowest order of the real-space perturbation theory for quantum [18, 19] and thermal [20] fluctuations. Below we present the opposite effect of *order by structural disorder*. We show that a small finite concentration of weak vacancies may be described by a positive biquadratic exchange $+(\mathbf{S}_i \cdot \mathbf{S}_j)^2$ in an effective spin Hamiltonian. Therefore, structural disorder stabilizes the least collinear spin configurations, which in the case of the TAFM correspond to conical states, and competes with conventional order by disorder mechanism.

For analytic derivation we need to modify the model for impurities, introduced in Eq. (1). As was discussed in the previous section, a true vacancy produces a strong long-range distortion of the surrounding spin structure. Therefore, below we restrict ourselves to a model of weak classical impurities with reduced spin length $\mathbf{S}_i(1 - \varepsilon p_i)$, and $\varepsilon \ll 1$. This approximation is analogous to restricting the impact of impurities to its nearest neighbors only, as illustrated in Fig. 1(a). Numerical results of our previous work [12] demonstrate that this approximation does not affect the conclusion. Therefore, we expect the state selection produced by real vacancies to be even more robust.

In the following we follow the ideas of the real-space perturbation theory [18–20]. We start at $T = 0$ with an arbitrary classical ground state of the pure system and express the Hamiltonian in terms of small spin deviations, caused by impurities. Then, we collect all single-site terms and find a static distortion of the equilibrium magnetic structure from a simple minimization procedure. The remaining terms, that represent interaction of perturbations, will be neglected, as they produce higher-order corrections [14].

An arbitrary classical ground state of the pure system is characterized by a set of angles θ_{ij} between neighboring spins. Performing transformation to a local rotating frame we obtain

$$\hat{\mathcal{H}} = J \sum_{\langle ij \rangle} \left[S^y_i S^y_j + \cos\theta_{ij} \left(S^z_i S^z_j + S^x_i S^x_j \right) + \sin\theta_{ij} \left(S^z_i S^x_j - S^x_i S^z_j \right) \right] \left[1 - \varepsilon(p_i + p_j) \right] + \hat{\mathcal{H}}_{\rm Z}. \quad (6)$$

The local $\hat{\mathbf{z}}_i$ axes are chosen along the spin direction on each site, whereas the $\hat{\mathbf{x}}_i$ axes lie

within the plane, formed by a pair of spins $\mathbf{S}_i$ and $\mathbf{S}_j$. Impurities produce distortions of the spin structure, generating small transverse components components of spins S^x and S^y that correspond to in plane and out of plane spin deviations. Then one can write

$$S^z = \sqrt{1-(S^x)^2-(S^y)^2} \approx 1 - \frac{1}{2}[(S^x)^2) + (S^y)^2] \tag{7}$$

All terms arising from interaction of spin deviations on adjacent sites are neglected. Therefore the leading ground-state energy correction comes from the contribution that is linear in in-plane spin deviations S^x and disorder ε

$$V_1 = J\varepsilon \sum_{\langle ij \rangle} \sin\theta_{ij} \left(S_i^x p_j - S_j^x p_i \right). \tag{8}$$

Physically, terms linear in spin deviations appear due to a local relief of magnetic frustration caused by impurities. Excluding the out of plane spin components S^y that do not enter in V_1, and we are left with

$$\hat{\mathcal{H}} = \sum_i \left[\frac{1}{2} H_{\rm loc} (S_i^x)^2 + J\varepsilon S_i^x \sum_{j=1}^{6} \sin\theta_{ij} p_j \right]. \tag{9}$$

Here $H_{\rm loc} = |\partial E_{\rm g.s.}/\partial \mathbf{S}_i| = 3J$ is a local field, which is the same on all three sublattices of the pure TAFM irrespective of the applied field $H < H_{\rm sat}$. Minimizing this quadratic form, we obtain the correction to the ground state energy, generated by disorder. Note that throughout the derivation, we omitted all constant terms, concentrating only on the configuration-dependent correction.

$$\Delta E = -\frac{\varepsilon^2 n_{\rm imp}}{H_{\rm loc}} \sum_{\langle ij \rangle} \sin^2\theta_{ij} = \frac{\varepsilon^2 n_{\rm imp}}{3J} \sum_{\langle ij \rangle} (\mathbf{S}_i \cdot \mathbf{S}_j)^2. \tag{10}$$

Similarly to the case of bond disorder [12] we obtained, that realistic impurities in the TAFM favor the conical spin state with the smallest values of $\cos\theta_{ij}$, as spin relaxation from the least collinear configurations produces the largest energy gain. The realistic model, given by equation (1) produces the similar positive biquadratic exchange term as random bond disorder but in principle suits more to describe numerical simulations of Ref. [12] as well as experiments on doped frustrated systems. Finally, we note that the above derivation stays completely intact for the TAFM with a planar anisotropy considered in the very first work [9]. In this case the conical states are suppressed by the XXZ anisotropy in the spin Hamiltonian. Still, the classical degeneracy is present within the manifold of the coplanar states [9]. In this case a positive biquadratic exchange will stabilize an anti-Y sate in the whole range of magnetic fields [12].

4. Conclusions

In this work we have described two effects, which appear in the frustrated Heisenberg triangular antiferromagnet with a small but finite density of nonmagnetic impurities. First, we demonstrate that an effective impurity moment revealed in the paramagnetic Curie tail of the magnetic susceptibility exhibits a substantial growth with the impurity concentration. We attribute this growth to an anomalously small value of the magnetic moment of an isolated vacancy in the TAFM, and, as a consequence, to significance of correlated impurity effects $\sim n_{\rm imp}^2$. This effect may be quantitatively different in other noncollinear helical antiferromagnets with not so small values of vacancy moments. Second, in the model of 'weak' impurities we have analytically derived an effective positive biquadratic exchange generated by the structural disorder. Such an interaction term competes with the effect of thermal and quantum fluctuations and plays a very important role in the phenomenology of the complex phase diagram of the doped TAFM [12]. With minor modifications, mainly in the value of $H_{\rm loc}$, the presented derivation holds for impurities in other geometrically frustrated magnets.

References

[1] Sachdev S, Buragohain C and Vojta M 1999 *Science* **286** 2479
[2] Sachdev S and Vojta M 2003 *Phys. Rev.* B **68** 064419
[3] Sushkov O P 2003 *Phys. Rev.* B **68** 094426
[4] Höglund K H, Sandvik A W and Sachdev S 2007 *Phys. Rev. Lett.* **98** 087203
[5] Eggert S, Syljuåsen O F, Anfuso F and Andres M 2007 *Phys. Rev. Lett.* **99** 097204
[6] Wollny A, Fritz L and Vojta M 2011 *Phys. Rev. Lett.* **107** 137204
[7] Wollny A, Andrade E C and Vojta M 2012 *Phys. Rev. Lett.* **109** 177203
[8] Chen C-C, Applegate R, Moritz B, Devereaux T P and Singh R R P 2011 *New J. Phys.* **13** 043025
[9] Lee D H, Joannopoulos J D, Negele J W and Landau D P 1984 *Phys. Rev. Lett.* **52** 433
[10] Kawamura H and Miyashita S 1985 *J. Phys. Soc. Jpn.* **54** 4530
[11] Gvozdikova M V, Melchy P-E, and Zhitomirsky M E 2011 *J. Phys.: Condens. Matter* **23** 164209
[12] Maryasin V S and Zhitomirsky M E 2013 *Phys. Rev. Lett.* **111** 247201
[13] Slonczewski J C 1991 *Phys. Rev. Lett.* **67** 3172
[14] Maryasin V S and Zhitomirsky M E 2014 *Phys. Rev.* B **90** 094412
[15] Lewtas H J, Boothroyd A T, Rotter M, Prabhakaran D, Müller H, Le M D, Roessli B, Gavilano J and Bourges P 2010 *Phys. Rev.* B **82** 184420
[16] Lüscher A and Sushkov O P 2005 *Phys. Rev.* B **71** 064414
[17] Chubukov A V and Golosov D I 1991 *J. Phys. Condens. Matter* **3** 69
[18] Long M W 1989 *J. Phys.: Condens. Matter* **1** 2857
[19] Heinilä M T and Oja A S 1993 *Phys. Rev.* B **48** 7227
[20] Canals B and Zhitomirsky M E 2004 *J. Phys.: Condens. Matter* **16** S759